Orbital Mediated Tunneling in Vanadyl Phthalocyanine Observed in both Tunnel Diode and STM Environments

K. W. Hipps,* Dan E. Barlow, and Ursula Mazur

Department of Chemistry and Materials Science Program, Washington State University, Pullman, Washington 99164-4630

Received: December 2, 1999; In Final Form: January 25, 2000

For the first time orbital mediated tunneling spectroscopy (OMTS) is reported for the same species, vanadyl phthalocyanine (VOPc), in both the tunnel diode and STM environments. IETS and OMTS for a junction of the form [Al−Al_2O_3−VOPc−Pb] show both the expected bias symmetry of vibrational and electronic inelastic electron tunneling spectroscopy (IETS) bands and the highly bias asymmetric OMTS band associated with tunneling via direct occupation of the Pc ring π^* orbital. STM studies of submonolayer coverage of VOPc on Au(111) produce well-resolved submolecular images of the molecule. Current imaging tunneling spectroscopy (CITS) allows one to easily identify VOPc islands, and the resulting I−V curves can be used to generate dI/dV spectra for VOPc and for bare gold regions. An intense band seen near +1.4 V bias (Au+) is identified as the same OMTS band as seen in the tunnel diode: resonance-like tunneling through the Pc ring π^* orbital.

Introduction

The presence of intense bias-asymmetric structure in the inelastic electron tunneling spectra (IETS) of metal−insulator−adsorbate−metal tunnel diodes was first observed by Mazur and Hipps.[1−4] They interpreted these structures as due to adsorbate orbital mediated elastic (or quasielastic) tunneling and identified these features as orbital mediated tunneling (OMT) bands. In their initial work, processes associated with the lowest unoccupied molecular orbital (LUMO) seemed to dominate, but they have recently reported OMT bands arising from occupied orbitals as well.[5] A model for predicting the approximate location of these OMTS bands based on electrochemical reduction and oxidation potentials was also proposed.[4] Subsequently, Tao and Lindsay have observed enhanced tunneling intensity in solution phase STM work located at potentials appropriate for electrochemical transformations of the porphyrins studied.[6−8] This redox enhanced tunneling had been predicted on theoretical grounds by Schmickler[9] for true resonance processes, and by Kuznetsov[10] in the case where there is relaxation of the intermediate ion before the electron is transferred to the opposite electrode. This issue of direct resonant tunneling versus electron hopping with the molecular ion being an intermediate state is still not resolved. It is of course quite difficult to unravel in solution where solvent reorganization and the rapid variation in potential in the double layer are complicating factors. It is presumed that all of these processes would fall under the general topic of orbital mediated tunneling (OMT).

For the first time, we present the OMTS of a compound in both the tunnel diode and STM environment. Unlike the studies of Lindsay and of Tao, we report UHV−STM results that should be more directly comparable with the tunnel diode environment.

Experimental Section

Al−Al_2O_3−VOPc−Pb tunnel diodes were fabricated by the same methods as were employed for other OMTS studies.[5] The VOPc was sublimed before use and was deposited to an average thickness of 0.4 nm as determined by a quartz crystal microbalance. Tunneling spectra were collected as normalized tunneling intensities (NTI), which are equivalent to (dσ/dV)/σ, where σ is the conductance of the device, dI/dV.[11,12] As is customary with IETS data, a low order polynomial was fit to the data and subtracted from it in order to remove the nonresonant elastic tunneling contributions. The NTI spectra reported here were measured at 4 K with a modulation voltage of 10 mV rms and are the sum of 36 scans.

The sample used for the STM study was prepared as follows. Freshly prepared Au(111) grown on mica was transferred into the UHV chamber housing a McAllister STM and a fixture for depositing VOPc. The compound was deposited on the gold to a thickness of about 0.2 nm as determined by a thin film monitor. The sample was allowed to cool and was placed on the STM stage. Both etched W and cut PtIr tips were used. The imaging and CITS were performed using Digital Instruments Nanoscope III software (version 3.31 − later versions do not perform CITS correctly) and control electronics. The only data manipulation performed upon the STM images were zoom and plane-fit. All STM data were acquired at room temperature.

I−V curves were extracted from the CITS data set using Nanoview version 1.1.[13] I−V curves were averaged over the majority of the VOPc covered region to produce a single I−V curve representative of the compound. Averaging simply consisted of adding together all the I(V) curves acquired over a given area and then dividing by the number of curves. Similarly, I−V curves were averaged over the majority of the clean Au surface to produce the I−V curve representative of the uncovered surface.

Note that many STM images and IETS spectra were taken of several samples. Images, spectra, and I−V curves are all reproducible.

Results

Figure 1 displays the baseline corrected NTI spectrum of a typical Al−Al_2O_3−VOPc−Pb tunnel junction at 4 K. The sharp

* Corresponding author e-mail: hipps@wsu.edu.

10.1021/jp994248q CCC: $19.00
Published on Web 02/23/2000

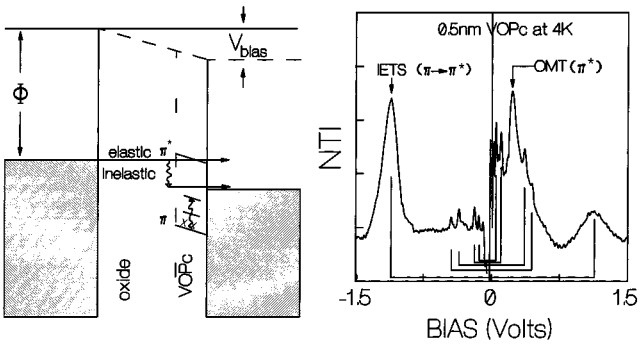

Figure 1. Schematic diagram of inelastic and resonant elastic tunneling processes (left). Tunneling spectroscopy data obtained from an Al−Al_2O_3−VOPc−Pb tunnel junction at 4 K with 10 mV rms modulation. Vertical lines guide the eye to the inelastic excitations that occur in both bias directions. The OMTS band associated with transient reduction of the Pc ring, on the other hand, appears only on the Pb+ bias side.

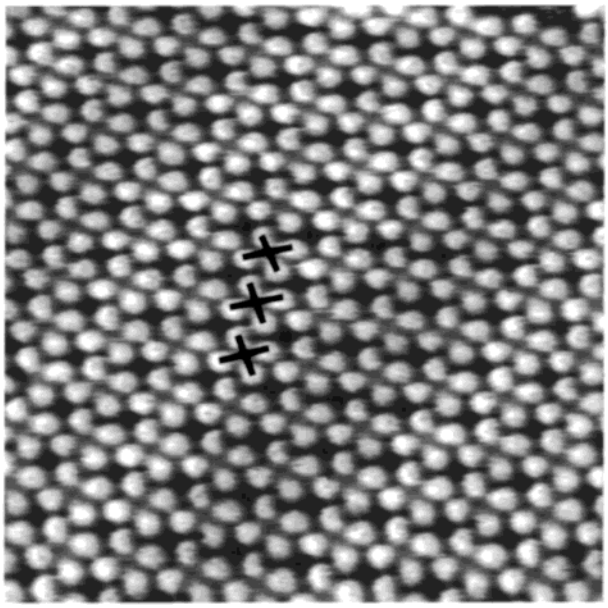

Figure 2. High resolution constant current image of VOPc on Au(111). Image is 13.6 nm × 13.6 nm and the gray scale is 0.3 nm. Sample was biased at +0.8V relative to the tip and the tunneling current was set at 0.3 nA and the temperature was held near 293 K. A Pt/Ir cut tip was used.

narrow features that occur in both positive (Pb+) and negative (Pb−) bias are due to inelastic vibrational excitations of the VOPc, while the intense broad features near ±1.1 V are due to inelastic electronic excitation of the $\pi\pi^*$ singlet to triplet transition of the Pc ring.[1,14,15] Note that 1 eV = 8066 cm^{-1}, so the mid-IR region extends to ±0.5 V bias. In addition to these inelastic features, there is a broad intense differential like feature with a peak apparent only in positive bias near 0.23 V. This latter feature is similar to structure seen in other metal phthalocyanines (MPcs) and has been attributed to direct quasielastic tunneling via reduction of the Pc ring.

A high resolution STM image of a single molecule thick island of VOPc on Au(111) is shown in Figure 2. We have identified three molecules by crosses to help guide the eye. Note that while the benzene rings of the Pc are very well defined, the nitrogens and central VO are not observed. This result should be contrasted with the images seen for CuPc and NiPc where the metal ions are not observed and for CoPc and FePc where the central metal ions are the tallest features in the image.[16,17] The interpretation of the apparent height contour of VOPc as seen by STM will be presented in a separate work.[18] Figure 3 (left image) is an STM image of a 250 nm × 250 nm region of the gold surface. On the upper right is an island of VOPc (as known from high resolution imaging), while the remainder of the surface is uncovered gold. The plateau on the left results from a single atomic gold step. Also seen in Figure 3 (right image) is the current image of the same area obtained from the CITS[19] data at +1.4 V. Here the chemical information dominates the structural data. Note that all of the gold surface is dark independent of the height, while the VOPc island is very bright. That is, the tunneling current is significantly enhanced by the presence of the VOPc.

If one averages the I−V curves obtained over the VOPc island, and also averages I−V curves from an equal area over the bare gold, very reliable and low noise curves result. These are shown in Figure 4 without any smoothing or modification. Spectroscopic data, in the form of dI/dV is extracted from the I−V curves in one of two ways. Curve 4A results when the VOPc/Au I−V curve is first smoothed and then differentiated, while curve 4B is obtained by differentiating an 18-parameter polynomial fit to the I−V data. These two methods were used to assist in identifying which features are real and which are noise artifacts. Curve 4C is the dI/dV resulting from differentiation of the smoothed Au only I−V curve of Figure 4.

Discussion

The conceptual model for OMTS via a LUMO is shown by the schematic in Figure 1. As the potential across the junction becomes more positive, the Fermi energy of the left-hand metal comes into energetic resonance with the unoccupied MO. Provided the total gap length (insulator + adsorbate) is large compared to the adsorbate thickness, a peak will be seen in the dI/dV curve at the energy of the LUMO.[20,21] Thus, the electron affinity of the adsorbate is equal to the work function of the right-hand metal minus the applied bias at which the peak in dI/dV occurs. In reverse bias, the LUMO never comes into resonance with the Fermi energy and no peak is seen.[22] In the NTI spectrum the OMT band takes on an asymmetrical derivative-like shape with the identifiable peak occurring somewhat below the maximum in dI/dV; the shift is approximately 0.1 V, which is of the order of the half width of the OMT peak seen in the NTI spectrum at an amplitude of 1/e of its maximum value.[20] Taking the work function of Pb to be 4.2 eV,[23] the position of the OMTS peak in Figure 1 to be 0.23 eV, and adding 0.08 eV (the 1/e half width of the peak), one obtains an electron affinity of 3.9 eV.

Turning next to the STM dI/dV spectra, we identify the peak near 1.4 eV bias as due to the same LUMO mediated process. Taking the work function of Au(111) to be 5.3 eV,[23] the electron affinity of VOPc is then 5.3 − 1.4 = 3.9 eV in rather remarkable agreement with the value obtained from the tunnel junction environment. *Thus, the OMT band seen in IETS at 4 K is also readily observed in dI/dV spectra in the UHV−STM environment at room temperature.*

In addition to the intense peak in dI/dV near 1.4 V bias in Figure 4, there is a weak but real rise in intensity near −1.1 V, and then a dramatic onset at the limit of our negative bias scan, −2 V. Comparing the IETS spectrum (Figure 1) and the dI/dV spectrum (Figure 4), it is tempting to assign the −1.1 V feature to inelastic scattering from the $\pi\pi^*$ transition of the Pc ring. Because this is an inelastic band, it should appear as a rounded step in dI/dV and be located at the same bias independent of the metal electrode.[14,15] Unfortunately, there is an alternative interpretation. It is equally likely that this feature is associated

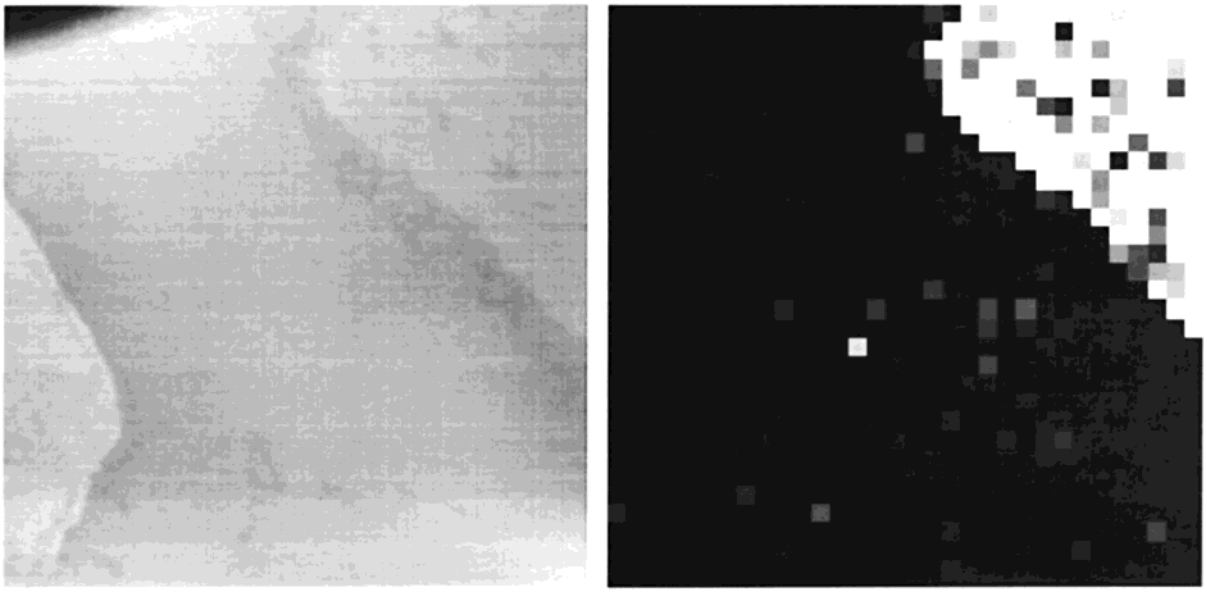

Figure 3. STM constant current image (left) and simultaneous CITS current image at 1.4 V sample bias (right) of the edge of a monolayer VOPc island (upper right in both figures). The images are 250 nm × 250 nm in the $x-y$ plane. The left image is drawn with a 1.0 nm gray scale while the right image has a 5 nA gray scale. The set point used was 0.3 nA and 800 mV.

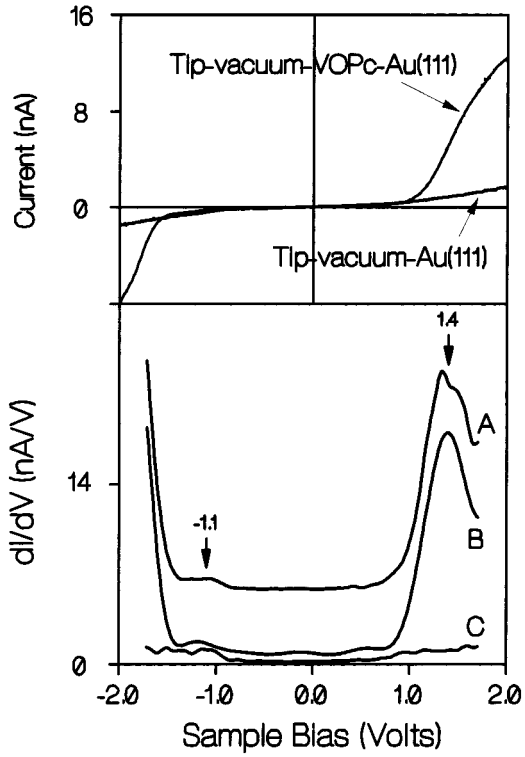

Figure 4. Area averaged IV and dI/dV curves taken from the CITS data set associated with Figure 3. The VOPc data was taken from the area average of the island on the right of Figure 3, while the bare Au data is an area average of the remaining surface. There are actually two curves identified as Tip−vacuum−VOPc−Au. A broken curve that is the actual data and a smooth curve that resulted form an 18-parameter least-squares polynomial fit to the data. dI/dV data were extracted from the IV curves. Numerical differentiation of the smoothed VOPc/Au I−V curve produced curve A. Differentiation of the fit to the VOPc/Au I−V data produced curve B. Numerical differentiation of the smoothed Au (only) I−V curve produced curve C. Curves A and B were offset by differing amounts for clarity of viewing.

with the density of states of the tip/substrate system since a similar (although less clear) rise in intensity occurs in the dI/dV of the VOPc free region of the surface (Figure 4C). At this time we have no assignment for the sharp increase in intensity at large negative bias, other than to note that it is probably due to some oxidative process and that it is almost certainly **not** the HOMO which should occur at least 0.5−1.0 eV higher in energy.[24−26] Clearly, however, this current enhancement involves some deeper occupied orbitals of the VOPc.

In comparing Figures 1 and 4, one may ask about the absence of any of the inelastic vibrational structure. The line width in IETS is limited by the thermal broadening of the Fermi level and amounts to about 5 kT.[14,15] At 300 K this corresponds to 0.15 eV. Thus, all of the vibrational structure is washed away and only the most intense electronic IETS and OMTS bands may be seen in dI/dV. Additionally, it should be recalled that IETS bands appear as rounded *steps* in dI/dV, while the OMTS bands appear as *peaks*.

The high degree of agreement between electron affinity values obtained from the tunnel junction and from STM is probably due, in part, to the fact that both lead and gold interact rather weakly with the Pc ring. If there were chemisorption on either of the metals, one would expect the electron affinities to reflect that interaction. We also expect the affinity values to change with sample thickness, since the effect of image charges in the metal (that stabilize the ionized molecule) diminish with increasing distance from the metal surface. Of course, the agreement may also be due to fortuitous cancellation of terms. There are certainly features of the interpretation of these spectra that we do not yet understand. For example, changing the tip material from Pt/Ir to W does not produce an appreciable peak shift. Thus the energy of the LUMO appears to be tied to the work function of the Au surface and not the average work function of the tip−VOPc−Au system. This is an interesting finding since in some cases, even in UHV, it is possible that adatoms may be present at the end of the tip and therefore produce spectra that are strongly tip dependent.

This first observation and interpretation of orbitally mediated tunneling bands in both tunnel junctions and in STM justifies the search for a unified theory of tunneling spectroscopy intensities and image contrast mechanisms in the STM of electroactive materials. Moreover, OMTS can now be used in both environments to experimentally determine electron affinities for adlayers on metal surface.

Acknowledgment. We thank the National Science foundation for support in the form of grants CHE 9709273, and CHE 9819318. Acknowledgment is also made to the donors of the Petroleum Research Fund, administered by the ACS, for partial support of this research.

References and Notes

(1) Hipps, K. W. *J. Phys. Chem.* **1989**, *93*, 5958−5960.
(2) Mazur, U.; Hipps, K. W. *J. Phys. Chem.* **1994**, *98*, 5824−5829.
(3) Mazur, U.; Hipps, K. W. *J. Phys. Chem.* **1994**, *98*, 8169−8172.
(4) Mazur, U.; Hipps, K. W. *J. Phys. Chem.*, **1995**, *99*, 6684−6688.
(5) Mazur, U.; Hipps, K. W. *J. Phys. Chem.*, **1999**, *103*, 9721−9727.
(6) Tao, N. J. *Phys. Rev. Lett.* **1996**, *76*, 4066−4069.
(7) Han, W.; Durantini, E. N.; Moore, T. A.; Moore, A. L.; Gust, D.; Rez, P.; Letherman, G.; Seely, G.; Tao, N.; Lindsay, S. M. *J. Phys. Chem. B* **1997**, *101*, 10719−10725.
(8) Schmickler, W.; Tao, N. *Electrochim. Acta* **1997**, *42*, 2809−2815.
(9) Schmickler, W. *J. Electroanal. Chem.* **1990**, *296*, 283−289.
(10) Kuznetsov, A.; Somner-Larse, P.; Ulstrup, J. *Surf. Sci*. **1992**, *275*, 52−64.
(11) Hipps, K. W.; Mazur, U. *Rev. Sci. Instrum.* **1988**, *59*, 1903−1905.
(12) Seman, T. R.; Mallik, R. R. *Rev. Sci. Instrum*. **1999**, *70*, 2808−2814.
(13) This excellent program is free and provided my Molecular Imaging Inc. We did correct a minor bug that causes currents to be read as half their true value.
(14) *Tunneling Spectroscopy: Capabilities, Applications, and New Techniques*; Hansma, P. K., Ed.; Plenum Press: New York, 1982; pp 229−269.
(15) Hipps, K. W.; Mazur, U. *J. Phys. Chem.* **1993**, *97*, 7803−7814.
(16) Lu, X.; Hipps, K. W.; Wang, X. D.; Mazur, U. *J. Am. Chem. Soc.* **1996**, *118*, 7197−7202.
(17) Lu, X.; Hipps, K. W. *J Phys. Chem. B*, 1997, *101*, 5391−5396.
(18) Barlow, D. E.; Hipps, K. W., submitted.
(19) Hamers, R. J. *Annu. Rev. Phys. Chem.* **1989**, *40*, 531.
(20) Hipps, K. W.; Mazur, U., submitted.
(21) Hamers, R. J. *J. Phys. Chem.* **1996**, *100*, 13103−13120.
(22) If the electroactive layer is thick or separated from both electrodes, this is not the case. See for example Sumi, H. *J. Phys. Chem. B* **1998**, *102*, 1833−1844; or reference 7.
(23) *CRC Handbook of Chemistry and Physics*, 68th ed.; CRC Press: Boca Raton, FL, 1988; E 89−90.
(24) Fischer, C. M.; Burghard, M.; Roth, S.; Klitzing, K. V. *Europhysics Lett.* **1994**, *28*, 375−378.
(25) Szuber, J.; Szczepaniak, B.; Kochowski, S.; Opilski, A. *Phys. Status Solidi B* **1994**, *183*, K9−K13.
(26) Lyons, L. E. *Aust. J. Chem.* **1980**, *33*, 1717−1725.